

CrossMark  
click for updatesCite this: *RSC Adv.*, 2016, 6, 34038

# Anhydrous proton conduction in liquid crystals containing benzimidazole moieties†

Shuai Tan, Bingzhuo Wei, Ting Liang, Xiaohui Yang and Yong Wu\*

A homologous series of biphenyl benzoate-based compounds with an alkthio chain bearing a benzimidazole moiety at the termini was synthesized by a nucleophilic substitution reaction. The compounds exhibited smectic A and nematic phases over a temperature range of 173–116 °C during the cooling process. A partially interdigitated bilayer order developed in the smectic assemblies and hydrogen-bonding between the benzimidazole moieties extended along the plane parallel to the smectic layer. Electrochemical characterization revealed that the liquid crystal phases favoured anhydrous proton conduction in the benzimidazole compounds and a proton conductivity of  $4.4 \times 10^{-5}$  S cm<sup>-1</sup> was achieved at 173 °C. The temperature dependence of the proton conductivities approximately followed the Arrhenius law and the proton conduction in the benzimidazole liquid crystals was assumed to be dominated by the proton hopping mechanism.

Received 5th February 2016  
Accepted 28th March 2016

DOI: 10.1039/c6ra03375j

www.rsc.org/advances

## Introduction

Anhydrous proton conductors for fuel cells working at intermediate temperatures (100–200 °C) have attracted much attention for the potential to promote cell performance.<sup>1–3</sup> Hydrogen-bonding networks formed by protonic moieties are believed to provide pathways for proton conduction in organic materials.<sup>4</sup> Amphoteric nitrogen-heterocycles such as imidazole, benzimidazole and triazole are regarded as candidates for anhydrous proton conductors because they can participate in hydrogen-bonding as both hydrogen bond donors and acceptors.<sup>5–11</sup> Jannasch *et al.* have reported proton conductivities of  $10^{-5}$  S cm<sup>-1</sup> at 160 °C for ethylene oxide oligomers tethered to benzimidazole units.<sup>7</sup> It was suggested that proton conduction in the heterocycle compounds occurred through structural diffusion and local mobility of the heterocycles would facilitate the process.<sup>6–9</sup> Comb polymers, acid–base complexes and porous coordination polymers have been proposed to construct well-ordered hydrogen-bonding pathways for the purpose of enhancing proton conduction in the heterocycle compounds.<sup>12–15</sup>

Liquid crystals have been adopted to obtain regular proton conducting pathways in some sulfonic compounds by virtue of their intrinsic order and fluidity,<sup>16–19</sup> but there are hardly any reports on nitrogen-heterocyclic liquid crystals for proton conduction. Basak *et al.* obtained a liquid crystal phase using

a triphenylene core with alkyl chains bearing a triazole moiety at their termini.<sup>20</sup> The exact arrangement of the triazole moieties in the liquid crystal phase remained unclear for the absence of informative X-ray scattering pattern. They found that the liquid crystal phase lowered the activation energy barrier for proton conduction and the maximum conductivity reached  $1 \times 10^{-5}$  S cm<sup>-1</sup> at 140 °C. Chen *et al.* have incorporated benzimidazole moieties into biphenyl mesogens to prepare three series of smectic liquid crystals.<sup>21</sup> However, the rigid mesogens might restrict reorientation of the nitrogen-heterocycles necessary for structural diffusion and the authors did not carry out any electrochemical characterization.

With a view to obtaining enhanced anhydrous proton conduction through nitrogen-heterocyclic liquid crystals, we synthesized a homologous series of benzimidazole compounds

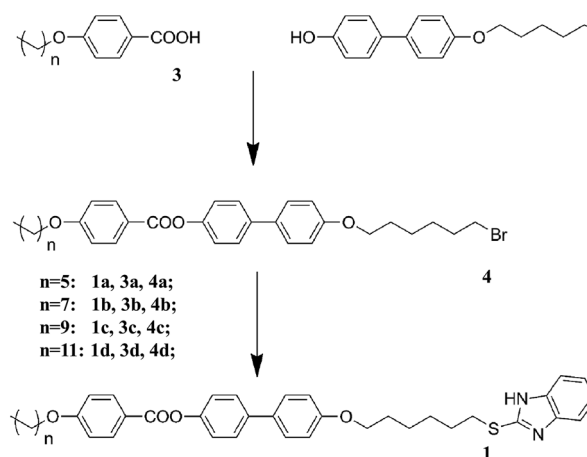


Fig. 1 Synthetic route of 1.

College of Chemical Engineering, Sichuan University, No. 24 South Section 1, Yihuan Road, Chengdu 610065, China. E-mail: wuyong@scu.edu.cn; Fax: +86 28 85403397; Tel: +86 28 85467527

† Electronic supplementary information (ESI) available: <sup>1</sup>H NMR spectra, FT-IR spectra, DSC curves, XRD patterns, impedance spectra and current relaxation curves. See DOI: 10.1039/c6ra03375j

as shown in Fig. 1. A rod-shaped biphenyl benzoate mesogen was employed to induce liquid crystal phases. A flexible alkoxy spacer between a terminal benzimidazole moiety and the mesogen assured local mobility of the nitrogen-heterocycle. A terminal alkoxy chain (containing carbon number from 6 to 12) on the other side of the mesogen harmonized rigidity and flexibility of the molecule. The objective benzimidazole compounds exhibited thermotropic nematic and smectic A phases during the cooling process. Hydrogen-bonding between the benzimidazole moieties formed lamellar networks owing to the bilayer smectic order. Electrochemical impedance spectroscopy (EIS) measurements revealed that the liquid crystal phases favoured anhydrous proton conduction in the benzimidazole compounds. The smectic benzimidazole liquid crystals provided an optional strategy to develop anhydrous proton conductors from nitrogen-heterocycles.

## Experimental

### General

The  $^1\text{H}$  nuclear magnetic resonance (NMR) spectra were measured by using a Bruker AV II-400 spectrometer. The Fourier transform infrared (FT-IR) spectra during the cooling process were obtained by a Nicolet 6700 spectrometer equipped with a Linkam hot stage. The sample was sandwiched between two ungreased ZnSe disks. Elemental analyses were done by using a Euro EA3000 CHNS/O Elemental Analyzer. The differential scanning calorimetry (DSC) measurements were performed by a TA DSC Q20 modulated instrument under a nitrogen atmosphere. The heating and cooling rates were  $10\text{ }^\circ\text{C min}^{-1}$ . Polarized optical microscopies (POM) of thin films were performed using a Weitu XPL-30TF equipped with a WT-3000 hot-stage. The X-ray diffraction (XRD) analyses were conducted on a Bruker AXS D8 discovery diffractometer equipped with a Hi-Star 2D detector, using Cu-K $\alpha$  radiation filtered by cross-coupled Göbel mirrors at 40 kV and 40 mA. Sample's temperature was controlled by an Anton Parr hot-stage. The EIS measurements were carried out using an electrochemical workstation consisting of an EG&G Princeton Applied Research (PAR) potentiostat/galvanostat model 273A and PAR lock-in-amplifier model 5210 connected to a PC running electrochemical impedance software (frequency range: 100 kHz to 0.1 Hz, applied voltage: 10 mV). The Wagner's direct current (DC) polarization<sup>22</sup> was measured using the same electrochemical workstation with direct current DC power supply (applied voltage: 0.85 V).

### Materials

All commercially-available starting materials, reagents and solvents were used as supplied and were obtained from TCI, Acros and Chengdu Changzheng. All reactions were carried out under a dry nitrogen atmosphere. The synthetic route of 4'-(6-(benzimidazolethio)hexoxy)-biphenyl-4-yl 4-(alkoxy)benzoate (**1**) is presented in Fig. 1. Compounds **2** and **3** were synthesized according to the procedures described previously.<sup>23,24</sup>

**Synthesis of 4'-(6-bromohexoxy)-biphenyl-4-yl 4-(alkoxy)benzoate (4).** All of these compounds were prepared by

procedures analogous to that described below for **4a**. **3a** (1.9 g, 8.6 mmol) was dissolved in thionyl chloride and stirred at room temperature for 30 min. The excess thionyl chloride was removed under reduced pressure and 4-hexoxy benzoyl chloride was obtained. Triethylamine (1.8 mL, 12.9 mmol) was added into a flask containing **2** (3 g, 8.6 mmol) in dichloromethane. The solution was stirred at room temperature for 30 min. 4-Hexoxy benzoyl chloride dissolved in dichloromethane was added dropwise into the solution. The mixture was stirred at room temperature for 5 h. After the reaction, the mixture was concentrated under reduced pressure. The residue was crystallized from methanol for twice and purified by flash column chromatography (silica) using dichloromethane as an eluent. **4a** (3.0 g) was obtained in 63% yield.  $^1\text{H}$  NMR (400 MHz,  $\text{CDCl}_3$ ): 8.16, 7.57, 7.51, 7.23, 6.97 (m, 12H, Ph), 4.01 (m, 4H,  $\text{PhOCH}_2$ ), 3.44 (t, 2H,  $\text{CH}_2\text{Br}$ ), 1.75–1.24 (m, 16H,  $\text{CH}_2\text{CH}_2$ ), 0.87 (t, 3H,  $-\text{CH}_3$ ). FT-IR  $\nu$ : 2932, 2861, 1725, 1606, 1513, 1498, 1470, 1389, 1258, 1212, 1163, 1072, 996, 880, 846, 791, 761, 728, 692, 651, 551 (C–Br), 513. For **4b**: yield: 61%. For **4c**: yield: 63%. For **4d**: yield: 62%.

**Synthesis of 4'-(6-(benzimidazolethio)hexoxy)-biphenyl-4-yl 4-(alkoxy)benzoate (1).** All of these compounds were prepared by procedures analogous to that described below for **1a**. 2-Mercaptobenzimidazole (1.0 g, 6.7 mmol) in aqueous NaOH solution ( $3.4\text{ mL}$ ,  $2\text{ mol L}^{-1}$ ) was stirred at room temperature for 30 min. **4a** (3.7 g, 6.7 mmol) dissolved in tetrahydrofuran (5 mL) was then added dropwise into the solution. The mixture was stirred at reflux for 8 h. After cooling, the mixture was evaporated under reduced pressure and the residue was extracted with water. The crude product was recrystallized from ethanol for twice and purified by flash column chromatography (silica) using dichloromethane as an eluent to give **1a** (3.8 g) as a white solid. Yield: 91%.  $^1\text{H}$  NMR (400 MHz,  $\text{CDCl}_3$ ): 8.16, 7.57, 7.51, 7.23, 6.97 (m, 16H, Ph), 4.01 (m, 4H,  $\text{PhOCH}_2$ ), 3.37 (t, 2H,  $\text{CH}_2\text{S}$ ), 1.75–1.24 (m, 16H,  $\text{CH}_2\text{CH}_2$ ), 0.87 (t, 3H,  $-\text{CH}_3$ ). FT-IR  $\nu$ : 3070, 2932, 2861, 1725, 1606, 1513, 1498, 1470, 1440 (C–S), 1389, 1344 (C=N), 1258, 1212, 1163, 1072, 996, 880, 846, 791, 761, 735, 682, 651, 519. Elemental analysis calcd (%) for  $\text{C}_{38}\text{H}_{42}\text{N}_2\text{O}_4\text{S}$  requires: C, 73.28; H, 6.80; N, 4.50; S, 5.15. Found: C, 73.31; H, 6.78; N, 4.48; S, 5.12. For **1b**: yield: 94%. Elemental analysis calcd (%) for  $\text{C}_{40}\text{H}_{46}\text{N}_2\text{O}_4\text{S}$  requires: C, 73.81; H, 7.12; N, 4.30; S, 4.93. Found: C, 73.77; H, 7.09; N, 4.33; S, 4.89. For **1c**: yield: 95%. Elemental analysis calcd (%) for  $\text{C}_{42}\text{H}_{50}\text{N}_2\text{O}_4\text{S}$  requires: C, 74.30; H, 7.42; N, 4.13; S, 4.72. Found: C, 74.28; H, 7.38; N, 4.12; S, 4.74. For **1d**: yield: 91%. Elemental analysis calcd (%) for  $\text{C}_{44}\text{H}_{54}\text{N}_2\text{O}_4\text{S}$  requires: C, 74.75; H, 7.70; N, 3.96; S, 4.54. Found: C, 74.71; H, 7.71; N, 3.93; S, 4.57.

## Results and discussion

### Mesomorphic properties

Mesomorphism of **1** was characterized by POM observation, DSC and XRD measurements. Multiple peaks detected in DSC traces of **1** (Fig. S4 see ESI†) indicated appearance of mesophases. The mesophase types were identified by textures of POM observation. When **1** was cooled from isotropic liquid, nematic (N) phase was recognized from schlieren textures. On

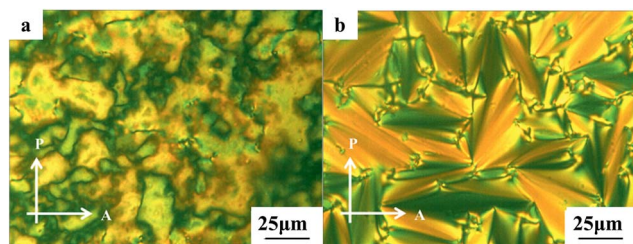


Fig. 2 Polarized optical micrographs of **1d** at 155 °C (a) and at 130 °C (b) during cooling ( $\times 400$ ). Direction of A: analyzer; P: polarizer.

Table 1 Phase transition temperatures and corresponding enthalpies derived from DSC traces<sup>a</sup>

Comps	Transition temperatures (°C) (enthalpy changes (kJ mol <sup>-1</sup> ))	$\Delta T_{LC}$ (°C)	
		S <sub>A</sub>	N
<b>1a</b>	C <sup>1st</sup> : I 173(0.8) N 133(5.9) S <sub>A</sub> 125(26.6) C	8	40
	H <sup>2nd</sup> : C 166(33.8) N 177(0.7) I	—	11
<b>1b</b>	C <sup>1st</sup> : I 170(0.9) N 129(0.5) S <sub>A</sub> 119(39.1) C	10	41
	H <sup>2nd</sup> : C 156(37.7) N 169(0.8) I	—	13
<b>1c</b>	C <sup>1st</sup> : I 162(0.8) N 146(0.9) S <sub>A</sub> 118(39.1) C	28	16
	H <sup>2nd</sup> : C 159(36.7) N 165(0.8) I	—	6
<b>1d</b>	C <sup>1st</sup> : I 159(0.8) N 146(1.0) S <sub>A</sub> 116(38.2) C	30	13
	H <sup>2nd</sup> : C 157(37.0) N 162(1.0) I	—	5

<sup>a</sup> Note: C, solid; I, isotropic liquid; C<sup>1st</sup>, first cooling; H<sup>2nd</sup>, second heating;  $\Delta T_{LC}$ , temperature range of a liquid crystal phase.

further cooling, smectic A (S<sub>A</sub>) phase was discerned from focal conic textures. Only N phase was observed when **1** was heated from solid to isotropic liquid state. Representative POM textures observed for **1** are presented in Fig. 2. Phase transition temperatures and enthalpy changes derived from the DSC traces are listed in Table 1. The longer alkoxy chain resulted in the broader temperature range of the S<sub>A</sub> phase because of the enhanced laterally intermolecular forces of attractions.<sup>25</sup>

Temperature dependent XRD measurements of **1** further confirmed the presence of the S<sub>A</sub> phase. The XRD pattern of **1d** at 130 °C during cooling is shown in Fig. 3. A sharp peak centered at  $2\theta = 1.1^\circ$  indicated a lamellar structure with a  $d$ -spacing of 7.8 nm. The spacing was longer than the length  $L$  of **1d** in the extended conformation (4.5 nm) and shorter than  $2L$ . Accordingly, a partially interdigitated bilayer order was assumed to develop in the smectic assembly. Essentially identical XRD patterns were also observed for **1a**, **1b** and **1c** (Fig. S5<sup>†</sup>). Meanwhile, intermolecular hydrogen-bonding between the benzimidazole moieties<sup>26</sup> was recognized from the broad absorption centered at 3070 cm<sup>-1</sup> in the FT-IR spectrum of **1d** at temperatures up to 160 °C (Fig. 4). Extended hydrogen-bonding networks have ever been observed in some benzimidazole self-assemblies<sup>13,21</sup> because the imidazole moieties participated in hydrogen-bonding both as donors and acceptors. Taking the XRD pattern and FT-IR spectrum into consideration, we inferred that side-by-side hydrogen-bonding between the benzimidazole moieties extended along the plane parallel to the smectic layer.

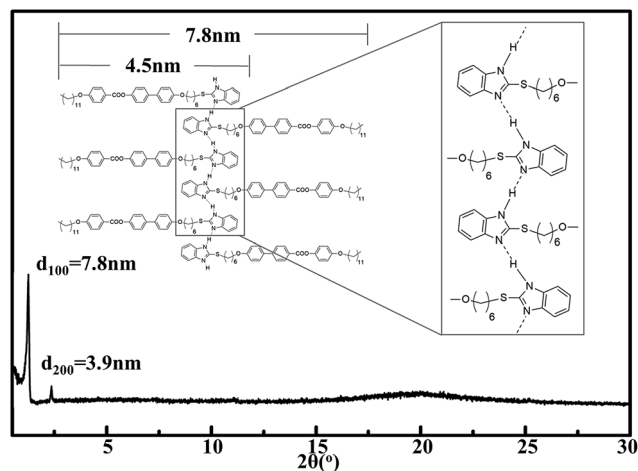


Fig. 3 XRD pattern of **1d** at 130 °C (inset is the proposed molecular packing mode in the S<sub>A</sub> phase).

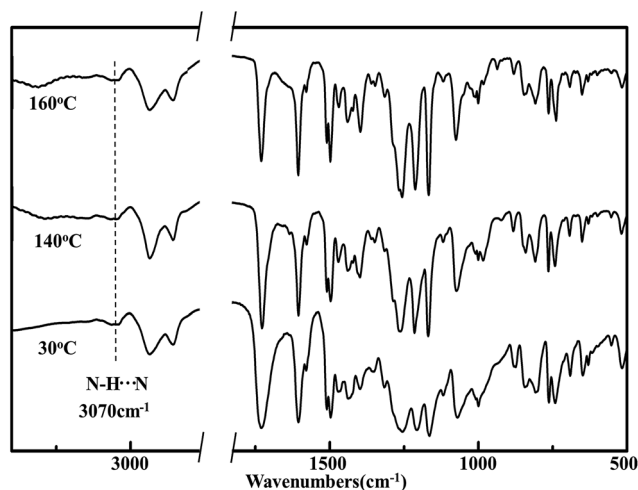


Fig. 4 FT-IR spectra of **1d** at 160, 140 and 30 °C during the cooling process.

The proposed molecular packing mode is schematically illustrated in Fig. 3. As a result, well-ordered pathways for proton conduction arose in the smectic assembly.

### Electrochemical characterization

EIS measurements were performed to determine proton conductivities (detailed measurement information was described in ESI<sup>†</sup>). The impedance responses obtained for **1** were characterized by the semicircles at high frequencies (Fig. S6 see ESI<sup>†</sup>), indicating occurrence of ionic conduction. The ionic transference numbers determined by the Wagner's DC polarization technique were 0.98–0.99 (Fig. S7 see ESI<sup>†</sup>), which suggested that ions were the predominant contribution to the conduction. Since diffusible ions other than protons did not exist in the compounds, the observed conductivities were reasonably ascribed to proton conductivities which could be calculated from the EIS responses and the cell constant (eqn (S2) see ESI<sup>†</sup>).

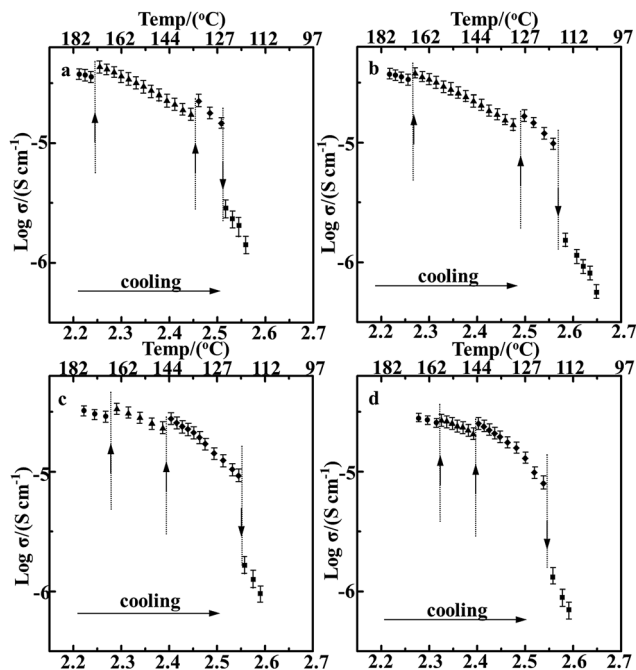


Fig. 5 Temperature dependent anhydrous proton conductivities of **1a** (a), **1b** (b), **1c** (c) and **1d** (d) during the cooling process (■ solid; ◆  $S_A$  phase; ▲ N phase; ● isotropic liquid).

The variation of the proton conductivity with temperature is shown in Fig. 5. The conductivities decreased with the decrease in temperature during the cooling process except for the  $I \rightarrow N$  and  $N \rightarrow S_A$  phase transition points. At the  $I \rightarrow N$  transition point, conductivities of **1** increased by 11% in average. The slight increase in proton conductivities should originate from the nematic order. Uniaxial arrangement of the benzimidazole molecules probably promoted formation of proton pathways. At the  $N \rightarrow S_A$  transition point, conductivities of **1** increased by 24% in average. The elevated proton conductivities were ascribed to the increased lamellar proton pathways induced by the smectic order. The abrupt increase in conductivities at the  $I \rightarrow N$  and  $N \rightarrow S_A$  phase transition points revealed that liquid crystal phases favoured anhydrous proton conduction in the benzimidazole compounds. Nevertheless, proton conductivities of **1** decreased by 85% in average at the  $S_A \rightarrow C$  transition point. The significant decrease in conductivities should be caused by the loss of both the bilayer arrangement of the molecules and local mobility of the benzimidazole moieties in solid state. Mass fraction of the benzimidazole moiety in the molecule also affected the resultant conductivities. At the same temperature, conductivities of **1** decreased slightly with the increase in the length of the alkoxy chains. For example,  $\sigma$  values of smectic **1a**, **1b**, **1c** and **1d** at 125 °C were  $1.7 \times 10^{-5}$ ,  $1.6 \times 10^{-5}$ ,  $1.4 \times 10^{-5}$  and  $1.3 \times 10^{-5}$  S cm $^{-1}$ , respectively. The maximum conductivity achieved in the mesomorphic benzimidazole compounds was  $4.4 \times 10^{-5}$  S cm $^{-1}$ , which was higher than that of the reported mesomorphic triazole compound.<sup>20</sup>

The temperature dependence of conductivities in the N or  $S_A$  phases approximately followed the Arrhenius law (plot of  $\log \sigma$

Table 2 Activation energies of **1** in the mesophases obtained by the least-squares fitting

Comps	Activation energy $E_a$ (kJ mol $^{-1}$ ) (regression coefficient ( $R^2$ ))	
	$S_A$	N
<b>1a</b>	71.0(0.99)	38.4(0.99)
<b>1b</b>	70.8(0.99)	38.2(0.99)
<b>1c</b>	65.1(0.99)	36.0(0.99)
<b>1d</b>	69.0(0.97)	34.6(0.98)

versus  $T^{-1}$  (K $^{-1}$ ) is a straight line), which was quite different from the Vogel–Tamman–Fulcher mode<sup>27</sup> observed for some amorphous nitrogen-heterocycle compounds.<sup>6–8</sup> The proton conduction in these amorphous heterocycle conductors was assumed to be mediated by segmental motion of flexible chains. The Arrhenius behavior observed for **1** suggested that proton conduction in the benzimidazole liquid crystals was rather dominated by the proton hopping mechanism.<sup>28–30</sup>

The activation energies ( $E_a$ ) estimated from the Arrhenius plots (eqn (S3) see ESI $^\dagger$ ) are listed in Table 2.  $E_a$  for proton conduction in the  $S_A$  phase was approximately twice the value in the N phase. The positional restriction on molecules in the  $S_A$  phase might bring about additional energy barrier for proton exchange between the neighbouring benzimidazole moieties.

## Conclusions

Mesomorphic biphenyl benzoate-based compounds with an althio chain bearing a benzimidazole moiety at the termini were synthesized. The compounds exhibited thermotropic N and  $S_A$  phases during the cooling process. Lamellar hydrogen-bonding networks beneficial to anhydrous proton conduction developed in the smectic assemblies. The liquid crystal phases favoured anhydrous proton conduction in the benzimidazole compounds and conductivity of  $4.4 \times 10^{-5}$  S cm $^{-1}$  was achieved at 173 °C. The benzimidazole liquid crystals provided an optional strategy to prepare anhydrous proton conductors from nitrogen-heterocycles.

## References

- 1 K. A. Mauritz and R. B. Moore, *Chem. Rev.*, 2004, **104**, 4535.
- 2 Q. Li, R. He, J. O. Jensen and N. J. Bjerrum, *Chem. Mater.*, 2003, **15**, 4896.
- 3 J. A. Kerres, *J. Membr. Sci.*, 2001, **185**, 3.
- 4 K. D. Kreuer, *Chem. Mater.*, 1996, **8**, 610.
- 5 W. Münch, K. D. Kreuer, W. Silvestri, J. Maier and G. Seifert, *Solid State Ionics*, 2001, **145**, 437.
- 6 M. F. H. Schuster, W. H. Meyer, M. Schuster and K. D. Kreuer, *Chem. Mater.*, 2004, **16**, 329.
- 7 J. C. Persson and P. Jannasch, *Chem. Mater.*, 2003, **15**, 3044.
- 8 R. C. Woudenberg, O. Yavuzcetin, M. T. Tuominen and E. B. Coughlin, *Solid State Ionics*, 2007, **178**, 1135.
- 9 C. A. Alabi, Z. Chen, Y. S. Yan and M. E. Davis, *Chem. Mater.*, 2009, **21**, 4645.

- 10 C. Nagamani, C. Versek, M. Thorn, M. T. Tuominen and S. Thayumanavan, *J. Polym. Sci., Part A: Polym. Chem.*, 2010, **48**, 1851.
- 11 J. C. Persson and P. Jannasch, *Macromolecules*, 2005, **38**, 3283.
- 12 S. Bureekaew, S. Horike, M. Higuchi, M. Mizuno, T. Kawamura, D. Tanaka, N. Yanai and S. Kitagawa, *Nat. Chem.*, 2009, **8**, 831.
- 13 Y. Chen, M. Thorn, S. Christensen, C. Versek, A. Poe, R. C. Hayward, M. T. Tuominen and S. Thayumanavan, *Nat. Chem.*, 2010, **2**, 503.
- 14 D. Basak, C. Versek, J. A. Harvey, S. Christensen, J. Hillen, S. M. Auerbach, M. T. Tuominen and D. Venkataraman, *J. Mater. Chem.*, 2012, **22**, 20410.
- 15 M. Yamada and I. Honma, *J. Phys. Chem. B*, 2006, **110**, 20486.
- 16 S. Tan, C. Wang and Y. Wu, *J. Mater. Chem. A*, 2013, **1**, 1022.
- 17 T. Liang, Y. Wu, S. Tan and C. Wang, *J. Appl. Polym. Sci.*, 2014, **131**, 40382.
- 18 S. Tan, C. Wang, T. Liang, W. Huang and Y. Wu, *J. Mol. Struct.*, 2013, **1045**, 15.
- 19 B. Soberats, M. Yoshio, T. Ichikawa, S. Taguchi, H. Ohno and T. Kato, *J. Am. Chem. Soc.*, 2013, **135**, 15286.
- 20 D. Basak, S. Christensen, S. K. Surampudi, C. Versek, D. T. Toscano, M. T. Tuominen, R. C. Hayward and D. Venkatarama, *Chem. Commun.*, 2011, **47**, 5566.
- 21 L. Zhang, X. Chen, F. Zhao, X. Fan, P. Chen and Z. An, *Liq. Cryst.*, 2013, **40**, 396.
- 22 S. Selvasekarapandian, R. Baskaran and M. Hema, *Phys. B*, 2005, **357**, 412.
- 23 N. Kawatsuki, S. Sakashita, K. Takatani, T. Yamamoto and O. Sengen, *Macromol. Chem. Phys.*, 1996, **197**, 1919.
- 24 T. Kato and J. M. J. Fréchet, *J. Am. Chem. Soc.*, 1989, **111**, 8533.
- 25 M. A. Osman, *Z. Naturforsch.*, 1983, **38**, 693.
- 26 C. Perchard and A. Novak, *J. Chem. Phys.*, 1968, **48**, 3079.
- 27 M. A. Ratner, *Polymer Electrolyte Reviews*, Elsevier Applied Science, New York, 1987.
- 28 M. Armand, *Solid State Ionics*, 1983, **9**, 745.
- 29 R. Bouchet and E. Siebert, *Solid State Ionics*, 1999, **118**, 287.
- 30 J. T. Daycock, G. P. Jones, J. R. N. Evans and J. M. Thomas, *Nature*, 1968, **218**, 672.